Dissecting the mechanism regulating the activity of a conserved σ^{54}-dependent transcriptional activator in bacteria

A Report

submitted to

Indian Institute of Science Education and Research Pune in partial fulfilment of the requirements for the BS-MS Dual Degree Programme

by

Utkarsh Anil Mahajan



Indian Institute of Science Education and Research Pune

Dr. Homi Bhabha Road,

Pashan, Pune 411008, INDIA.

April 2022

Certificate

This is to certify that this dissertation entitled **"Dissecting the mechanism regulating the activity of a conserved σ^{54}-dependent transcriptional activator in bacteria"** towards the partial fulfilment of the BS-MS dual degree programme at the Indian Institute of Science Education and Research, Pune, represents study/work carried out by Utkarsh Anil Mahajan at the Indian Institute of Science Education and Research, Pune, under the supervision of Dr. Sunish Kumar Radhakrishnan, Associate Professor, Department of Biology during the academic year 2021-2022.



Utkarsh Anil Mahajan



Dr. Sunish Kumar Radhakrishnan

Department of Biology

IISER, Pune

Declaration

I hereby declare that the matter embodied in the report entitled **“Dissecting the mechanism regulating the activity of a conserved σ^{54}-dependent transcriptional activator in bacteria”** are the results of the work carried out by me at the Department of Biology, Indian Institute of Science Education and Research, Pune, under the supervision of Dr.Sunish Kumar Radhakrishnan and the same has not been submitted elsewhere for any other degree.



Utkarsh Anil Mahajan

TABLE OF CONTENT

Certificate..... 2

Declaration..... 3

Abstract.....6

Acknowledgements.....7

Introduction 8

Materials and Methods.....13

Results and Discussion.....18

Conclusion.....33

References.....34

LIST OF FIGURES

Figure 1: Life cycle of *Caulobacter crescentus*……...9

Figure 2: Phospho-transfer mechanism of TacA.....11

Figure 3: Motility assay of *ΔspmY* suppressors 12

Figure 4: Construction of *spmB* knockout plasmid .....……18

Figure 5: Screening for knockouts …….....19

Figure 6: Validation of knockouts…….....20

Figure 7: Phase-contrast microscopy images of knockouts……..22/23

Figure 8: Motility assay of knockouts…….....23

Figure 9: β-galactosidase activity assay in knockouts..... ……..24

Figure 10: Construction of SpmY-ALFA plasmid 25

Figure 11: Western blot showing the steady-state level of SpmY. 26

Figure 12: Immunoblot showing immunoprecipitated (IP) samples(Trial 1).....27

Figure 13: Immunoblot showing immunoprecipitated (IP) samples(Trial 2).....28

Figure 14: Native SpmY pulldown mass spectrometry result…….....29

Figure 15: SpmY-ALFA pulldown mass spectrometry result…….....30

Figure 16: Motility assay of *citA* mutants…….....32

ABSTRACT

In the dimorphic bacterial model, *Caulobacter crescentus* stalked and flagellated pole-specific localisation and activation of proteins leads to cell-fate determination and asymmetry during the cell cycle. For example, the initiation of the cell-fate determining signalling cascade begins with the stalked-pole specific localisation of the polar morphogen, SpmX, which in turn recruits and activates a set of proteins including the cell-fate determining kinase DivJ. The SpmX-mediated signalling negatively regulates the activity of the master cell cycle regulator, CtrA - through DivJ, and the σ^{54}-dependent transcriptional activator, TacA, through another polarised component SpmY. Deletion of *spmX* and/or *spmY* results in cell cycle and developmental defects shown to be caused by hyperactive TacA. However, the mechanism by which SpmX-SpmY regulates the activity of TacA still remains unclear. Herein, findings from a combination of genetic and biochemical experiments, have helped us gain preliminary insights into the possible signalling mechanism that SpmY might use to curb the activity of TacA is reported.

ACKNOWLEDGEMENT

I would like to extend my sincere and heartfelt thanks to all the people who have helped me in this endeavour. I am using this opportunity to express my deepest gratitude and special thanks to Dr. Sunish Kumar Radhakrishnan without his constant guidance, it would have been impossible to carry out this project.

I would also like to thank my TAC member Dr. Gayathri Pananghat for her valuable inputs and feedback which helped me improve my project.

I sincerely thank all the members of SKR Lab for their cooperation and help during these rather difficult times. I want to especially thank Unnimaya for guiding me through various hurdles and constantly inspiring me to do better.

Additionally, I would also like to thank Krishnendu for helping me with mass spectrometry sample preparation.

I would like to express heartfelt gratitude to my friends here at IISER, especially Aditi, Prajakta and Vibhor, for supporting me all along and making my experience at IISER Pune fun-filled and memorable.

I’m deeply indebted to my parents and especially to my brother Sham for always being there and making my life cheerful and filled with joy.

INTRODUCTION

Caulobacter crescentus, an alpha-proteobacterium with a dimorphic life cycle, is an extensively used model system to understand the cell cycle at its most fundamental level. Studies in *C. crescentus* have enhanced our understanding of the cellular process. Its dimorphic cell cycle makes it easy to dissect the properties of each phase and has added a plethora of things to our understanding of the bacterial internal architecture, cellular development, and cell-cycle control.

During each cell-division cycle, *Caulobacter crescentus* divides asymmetrically to give rise to two different types of cells with differential replicative and developmental fates. The swarmer cell is incapable of chromosomal replication and resides in the G1 phase. On the other hand, the stalked cell is capable of replication and division. The two daughter cells in *Caulobacter* can be distinguished easily using morphological and functional criteria: the G1-phase cell contains flagellum and pili at the swarmer pole, whereas the S-phase cell has an extension of the cell membrane known as stalk at the other pole. The swarmer cell, which is in the G1 phase, goes through an obligate differentiation into the stalked cell, which is in the S phase(Curtis and Brun, 2010). The G1 to S transition starts with the loss of pili and flagellum, along with the development of a stalk at the pole(Laub et al., 2007).

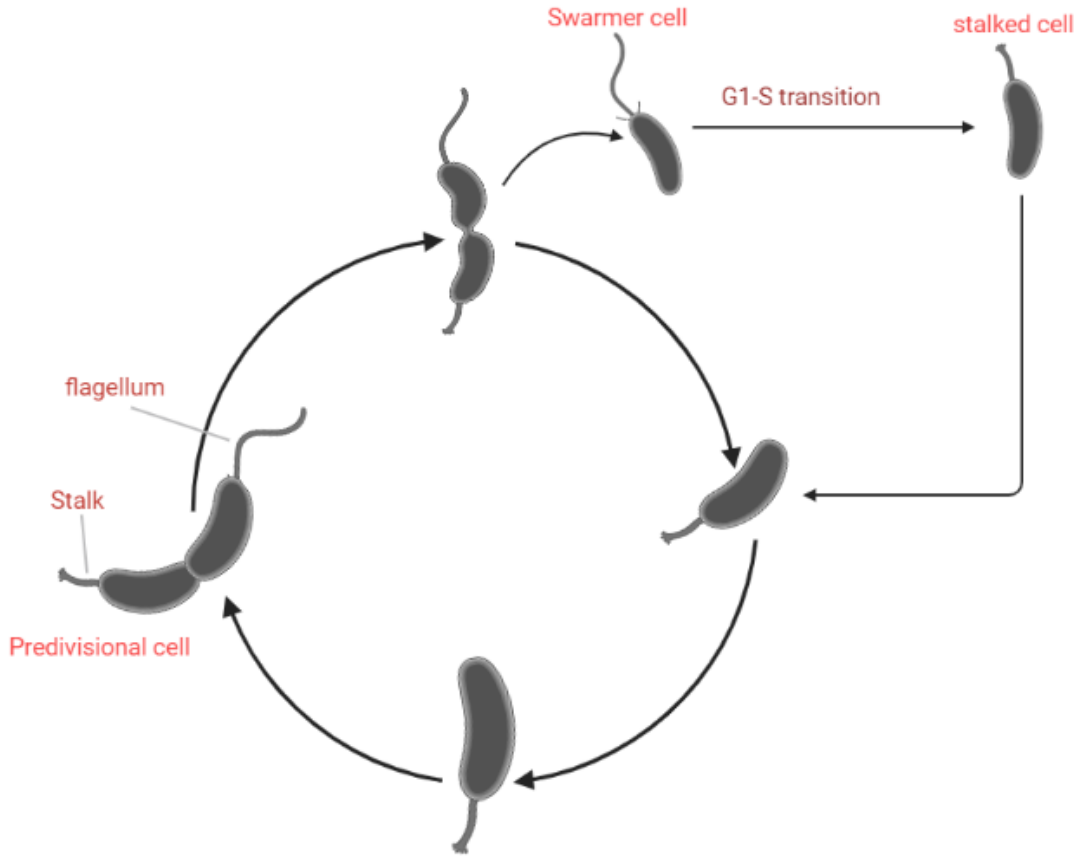


Figure 1: Cell cycle of *C. crescentus.* The cell cycle starts with the initiation of replication of the chromosome in the stalked cell as it enters the S phase. Simultaneously it grows and becomes a predivisional cell. A flagellum forms at the swarmer cell pole during the late predivisional stage, after which the predivisional cell gets separated, giving rise to two different kinds of cells. First, a stalked cell that re-enters the S phase starts DNA replication and continues the cyclical development. Second, the Swarmer cell, which is replication-incompetent, stays in the G1 phase. Afterwards, the swarmer cell enters the S phase by differentiating into the stalked cell.

The differential cell fate of the daughter cells is brought about by the asymmetric phosphorylation of the cell fate determinant DivK. In the stalked compartment of the predivisional cell, DivK is predominantly present in its active phosphorylated form (DivK~P), while in the swarmer cell compartment, it is present in the dephosphorylated form. The stalked-pole localised kinase, DivJ, is responsible for phosphorylating DivK in the stalked-pole compartment. The dephosphorylation of DivK is carried out by the phosphatase PleC localised at the swarmer cell pole (Jacobs et al., 2001; Matroule et al., 2004; Wheeler and Shapiro, 1999). The localisation and activation of the kinase DivJ, specifically at the stalked pole, is brought about by the stalked-pole specific developmental regulator SpmX (Radhakrishnan et al., 2008). The production and localisation of SpmX at the stalked pole during the swarmer to stalked cell transition helps to directly recruit and activate DivJ at the stalked pole, thereby triggering the production of DivK~P (Radhakrishnan et al., 2008).

DivK regulates the cell cycle through the transcriptional regulator CtrA (Hung and Shapiro, 2002; McGrath et al., 2006; Quon et al., 1996). The presence of CtrA is vital for cell survival, and the active form of CtrA, CtrA~P, activates many genes which are essential for cell division and development (Jacobs et al., 2001; Jonas et al., 2011; Laub et al., 2000). The master regulator, CtrA, inhibits replication initiation in the swarmer cells by binding to the chromosomal origin of replication(Jonas et al., 2011; Quon et al., 1998)(Jonas et al., 2011; Quon et al., 1998). DivK~P acts negatively on CtrA~P by downregulating its accumulation and thus inhibiting CtrA activated genes and relieving the repression of the replication origin, facilitating chromosome replication initiation (Quon et al., 1998).

Deletion of the *spmX* results in developmental defects in cells due to which *ΔspmX* cells are long with multiple constrictions at abnormal positions (Radhakrishnan et al., 2008). The *spmX* mutants are also non-motile. Additionally, *ΔspmX* cells have stalks at both poles, indicating a loss of asymmetry in these cells(Radhakrishnan et al., 2008). Surprisingly, it was discovered that not all the developmental defects of the *spmX* null mutant are due to perturbations in the DivJ/DivK phosphorelay pathway (Janakiraman et al., 2016). Furthermore, it was shown that SpmX, through another cell

cycle regulator SpmY, influences the activity of the σ^{54}-activator TacA and that an uncontrolled TacA activity contributes to the developmental defects of the *spmX* mutant (Janakiraman et al., 2016). SpmY is recruited to the stalked pole by SpmX through DivJ in the late S-phase(Janakiraman et al., 2016). Deletion of *spmY* resulted in the elevation of TacA activity, and the developmental defects (i) were independent of DivK-CtrA, and (ii) phenocopied a *spmX* null mutant (Janakiraman et al., 2016). These results indicated a significant role for SpmX-SpmY in fine-tuning the activity of TacA during the cell cycle in *Caulobacter*. Nevertheless, the underlying mechanism by which SpmY influences the activity of TacA remains to be elucidated. TacA is phosphorylated by the multicomponent phosphorelay in which Histidine kinase, ShkA, transfers phosphate to histidine phosphotransferase, ShpA, which transfers phosphate to TacA, thereby activating it (Biondi et al., 2006) (Figure 2).

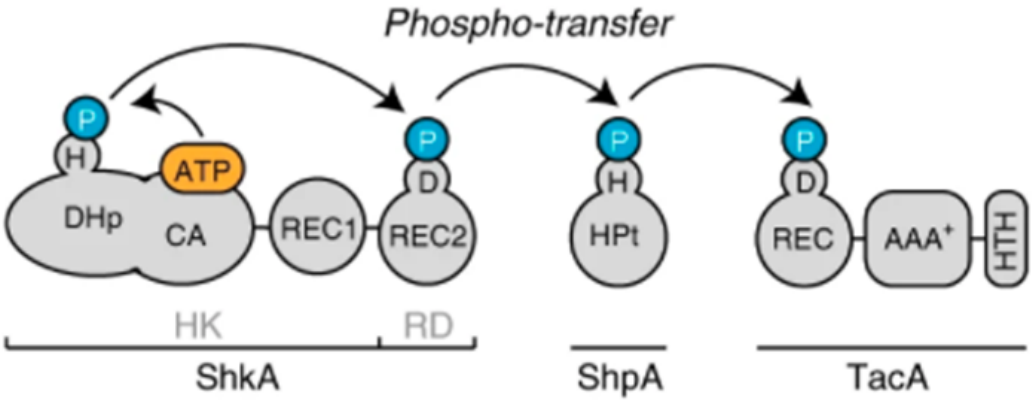


Figure 2: Schematic representation of the ShkA-ShpA-TacA phospho-transfer. The catalytic domain of the kinase, ShkA, binds to ATP and transfers phosphate to the histidine residue of the histidine-phosphotransfer domain (DHp), which gets transferred to the aspartate residue of the receiver domain (REC2) present at the C-terminal of protein. Phosphate is then transferred to another histidine phosphotransferase, ShpA, which finally transfers phosphate to aspartate residue present at the N-terminal of TacA [Image is adapted from (Kaczmarczyk et al., 2020)].

The primary objective of this work is to tease out the role of SpmY in decreasing levels of phosphorylated TacA (TacA~P), thereby restricting the activity of TacA to the early stages of the cell cycle. A motility-based genetic screen had led to the identification of the suppressors *spmA* and *spmB,* where it was demonstrated that transposon mutants of *spmA* and *spmB* could alleviate the motility defects of the *spmY* null mutant (Aravind and Radhakrishnan, unpublished).

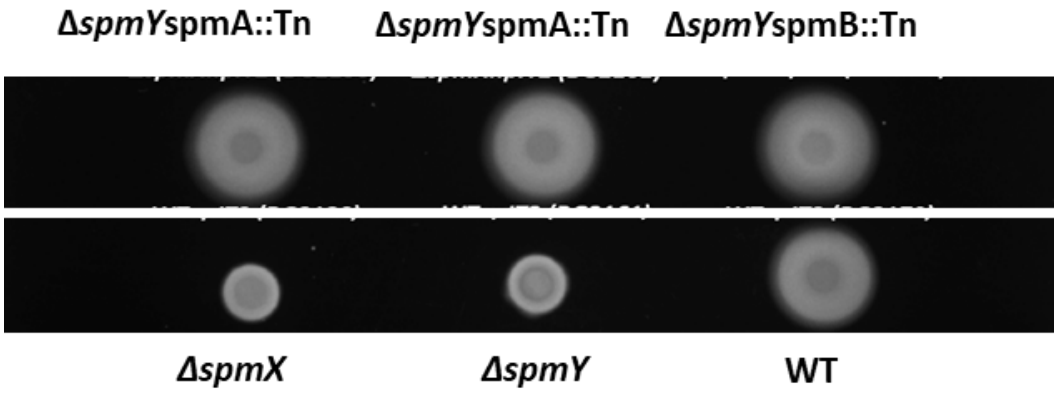


Figure 3: Soft agar plate showing motility of *ΔspmX*, *ΔspmY*, WT cells and the suppressor of *ΔspmY*, the *ΔspmYspmA*::Tn and the *ΔspmYspmB*::Tn in the top panel [Adapted from the thesis of Arvind Gopi].

In this work, experiments were carried out to (i) ascertain the role of SpmA and SpmB in regulating the activity of TacA and (ii) analyse the regulators that reside in a complex with SpmY, possibly influencing the activity of TacA.

MATERIALS AND METHODS

Cell culture and growth conditions:

C. crescentus cells were grown in PYE media at 29°C. *Escherichia coli* DH5α and d EC100 were used for cloning and were grown in LB at 37 °C. PYE-Agar plates contained 1.25% [w/v] agar. Motility was done on soft agar plates containing 0.3% agar.

Knockout plasmid construction:

To construct *the spmB* deletion plasmid two fragments were amplified. The first, a 650 bp fragment flanked on the 5' end by an EcoRI site and on the 3' end by a BglII site, spans the upstream region of *spmB* and extends 60 bp downstream of the start codon. The second 650 bp fragment was amplified so that it is flanked by Bgl II site at 5’ end and HindIII at 3’ end, including the final 60 bp of the *spmB* coding region and extended 586 bp downstream of the gene. After digesting with respective restriction enzymes, these fragments were ligated by three fragment ligation into pNPTS138 which was digested with EcoRI and HindIII.

Knockout strain construction:

Cells were electroporated with deletion plasmid and single recombinants were selected using kanamycin selection plates. Colonies were then grown in PYE broth and 100 µl of overnight grown culture was spread on a 3% sucrose plate to select for cells without plasmid. Colonies from sucrose plates were grown in PYE, followed by PCR of cell lysate to screen to confirm knockouts. DspmA_EF and DspmA_BR primers were used to screen for *spmA* knockouts and DspmB_BR and DspmB_ER primers were used for screening for *spmB* knockout.

SpmY-ALFA plasmid construction:

Plasmid pRXMCS2-P_{xyl}-spmY-ALFA was constructed by PCR sampling spmY using the genomic DNA of WT cells as a template. Which digested with NdeI and KpnI and then ligated into NdeI/Kpn1 digested pRXMCS2 plasmid. The positives clones were screened by isolating the plasmid and then digesting it to check for the presence of the expected fragment on the agarose gel.

β-Galactosidase assay:

The P_{spmX} -lacZ (Promoter of *spmX* transcriptionally fused with the *lacZ* reporter) containing cells were grown at 29°C grown in PYE-tetracycline(1 µg/ml) until OD is reached to 0.1-0.4 at 660 nm (A_{660}). One drop of chloroform was added to 50 µl of cells and vortex mixed to ensure that cells lysed properly.750 µl of Z-buffer (1 mM $MgSO_4.7H_2O$,60 mM Na_2HPO_4, 10 mM KCl,40 mM NaH_2PO_4,pH 7.0) was added to cell lysate. Ortho-Nitrophenyl-β-galactoside(ONPG) used as a substrate for this reaction. 200 µl of ONPG (4 mg/mL dissolved in 0.1M KPO_4 buffer [pH 7.0]) was added to the reaction mixture and the reaction was timed . At 30°C, the reaction mixture was incubated until a yellow colour appeared. The reaction was stopped by adding 500 µL of 1 M Na_2CO_3 solution. The absorbance of the supernatant was measured at 420 nm (A_{420}), Z-buffer was used as a blank in absorbance measurement . The miller units were determined using the formula,

$$U = \frac{A420 \times 1000}{A660 \times t \times v}$$

Where ‘U’ is miller units ,‘v’ is the culture volume (mL) and ‘t’ is the incubation time (min). The average of three independent experiments was used to calculate the experimental values. Statistical analysis was done using Prism 8 software.It was used to calculate the SEM indicated in the figures.

Generalised transduction:

Donor cells were grown overnight at 29°C. 10 µl of ϕCr-30 phage lysate is added to 600 µl of cell culture and incubated at room temperature for 10 min. It was added to 5 ml of soft agar and then poured on a PYE-agar plate. The plate was incubated at 29°C for 16-18 hours. The next day 5 ml of PYE was poured into the plate, followed by incubation at room temperature for 6 hours. Then PYE from the plate is collected in a 15 ml tube and 1 ml of chloroform is added, followed by centrifugation at 9000 RPM for 5 min at 4°C. Viral load was reduced by exposing it to UV in a UVP crosslinker. Then 100 µl phage lysate was added to 600 µl of overnight grown culture of recipient cells, followed by incubation at 29°C for 2 hours. Finally, it was selected by plating on kanamycin selection plates.

ALFA-tag pulldown:

The cells harbouring the spmY-ALFA plasmid were grown overnight and diluted in 500 ml of PYE-Kanamycin(5 µg/ml) and grown in the presence of 0.3% xylose. When OD 600 reached 0.6-0.8, cells were harvested by centrifugation at 8500 RPM at 4°C. Then the pellet was washed two times with PBS. Pellet was then resuspended into IP buffer I [50 mM Na_2HPO_4, 10 mM $MgCl_2$, 50 mM NaCl,1X protease inhibitor, 0.5% n-dodecyl-β-D-maltoside]. After that, 20 µl(250 units/µl) of lysozyme solution and 3 µl(10 units/µl) of DNaseI were added. Tubes were incubated at 37°C for 15 min to facilitate cell lysis. Pellet was then sonicated(3 seconds on, 5 seconds off, 70 % amplitude, 5 minutes), Followed by centrifugation at 10000 RPM for 5 min at 4°C. The supernatant was pre-cleared with 20 µl of washed control agarose resin beads (Thermo scientific). Then the ALFA Selector PE beads (NanoTag, Germany) were washed three times using IP buffer I. The supernatant was added to the beads and incubated at 4°C for 3 hours. After 3 hours tubes were centrifuged at 3000 RPM for 1 min at 4°C. Followed by the washing of beads twice with IP Buffer II (50 mM Na_2HPO_4, 50 mM NaCl, 1 mM EDTA, 1X protease inhibitor,0.5% n-dodecyl-β-D-maltoside) by adding 1 ml of IP Buffer II in a tube and incubating at 4°C followed by centrifugation at 3000 RPM for 1 minute. Beads were washed with IP buffer III (150 mM NaCl, 0.1%

n-dodecyl-β-D-maltoside,10 mM Tris-HCl[pH-8.0], 1X protease inhibitor) finally, beads were washed with 10% IP buffer III to remove salts. Then beads were resuspended in a 30 µL 4X SDS loading buffer, followed by mass spectrometry or Western blot analyses.

Mass Spectrometry:

Proteins from pulldown were allowed to migrate on 12.5 % SDS-PAGE gel. Protein bands were excised on a Coomassie-stained sodium dodecyl sulphate–polyacrylamide gel electrophoresis (SDS–PAGE) gel. The gel was cut into 1mm square pieces, and washed in a destaining buffer (40 % Acetonitrile, 50 mM Ammonium bicarbonate). Reduction was done by adding 10 mM dithiothreitol (DTT) to gel pieces and incubating for 30 min at 60°C. For alkylation, gel pieces were incubated in 20mM iodoacetamide (IAA) for 15 minutes at room temperature. After this 100% acetonitrile was added to dehydrate the gel pieces. Acetonitrile wash was repeated till the gel pieces were completely shrunken. 20 µl(0.5mg) of sequencing grade modified trypsin(Promega) was added to the gel pieces and allowed the gel pieces to rehydrate on ice for 1hr, followed by overnight incubation at 37C. After this, tubes were centrifuged and the supernatant was collected in a fresh tube. 200ul of 3% ACN/0.4% formic acid was added to the gel pieces and incubated for 10 min at RT, followed by transferring the supernatant to the tube to combine the digest. Then 200ul of 40% ACN/0.4% formic acid was added to gel pieces and after incubating for 10 min supernatant was collected. Finally, 100% ACN was added to gel pieces and the supernatant was collected. This process was repeated until the gel pieces were completely dehydrated. The supernatant was vacuum dried and then peptide fragments were resuspended in 0.1 % FA. The C_{18} column was used for desalting. The column was activated by adding 100 % ACN, followed by equilibration with 0.1% FA. Then peptides were loaded into the column washed with 0.1% FA and finally, peptides were eluted in 60% ACN/ 0.1% TFA.

Native SpmY pulldown:

NA100 cells were grown overnight at 29°C and diluted in 250ml of PYE. Cells were harvested when OD at 600 nm reached 0.5 - 0.7 by centrifugation at 8500 g. The pellet was washed two times in 1X PBS.Pellet was then resuspended into IP buffer II[50

mM $NaPO_4$ buffer [pH 7.4], , 10 mM $MgCl_2$, 50 mM NaCl ,1X protease inhibitor (Complete™ EDTA-free, Roche, Switzerland), 0.5% n-dodecyl-β-D-maltoside (Pierce, USA)]. After that, 20 µl(250 units/µl) of Ready-Lyse lysozyme solution (Lucigen, USA) and 3 µl(10 units/µl) of DNaseI (Roche, Switzerland) were added. After that, it was incubated at 37°C for 15 min to facilitate cell lysis., followed by centrifugation at 10000 RPM for 3 minutes at 4°C. The supernatant was pre-cleared with 30 µl of Protein-A beads (Roche), washed thrice in 1X PBS. Rabbit polyclonal anti-SpmY antibodies (1:500 dilution) were added to the precleared solution, followed by incubation at 4°C for 1.5 hours. The antibody-protein complex is then trapped using 50 µl of washed Protein-A agarose beads and incubated at 4°C for 1 hour. After incubation beads were washed with buffer I plus 0.5% n-dodecyl-β-D-maltoside, followed by washing twice with with 1% IP buffer (150 mM NaCl, 10 mM Tris-HCl[pH-8.0], 0.1% n-dodecyl-β-D-maltoside). Finally, beads were washed in 0.1% IP buffer to remove salts and resuspended in 50 µL 4X SDS loading buffer, followed by mass spectrometry or Western blot analyses.

Immunoblot:

The protein samples were resolved on 12.5 % sodium dodecyl sulphate polyacrylamide gel (SDS-PAGE) by applying constant voltage(100 V). Proteins were then transferred to a polyvinylidene difluoride membrane (PVDF) at 4°C. The membrane was blocked with 5 % milk in the TBST buffer (20 mM Tris-HCl [pH 7.5], 150 mM NaCl, 0.1% Tween-20) at room temperature for 1 hour. Blots were then incubated for 1 hour anti-SpmY antibodies(1:20,000 dilution) in TBST solution (20 mM Tris-HCl [pH 7.5], 150 mM NaCl, 0.1% Tween-20, 5% milk).Blots were then washed thrice with TBST buffer, followed by incubation of anti-rabbit secondary antibody. Blots were developed using Clarity Western ECL substrate(Biorad) and imaged on iBright FL1500 Imaging System (Thermo Fisher Scientific).

RESULTS

Deletion of *spmA* and *spmB* in *ΔspmY* and *ΔspmX* background

Given that transposon insertion in *spmB* and *spmA* were able to restore motility defects in *ΔspmY* cells(Figure 2). We made an in-frame deletion in the *spmB* in *ΔspmY* cells. To do so we constructed a *spmB* knockout plasmid by amplifying the upstream and the downstream region of the gene (Figure 4A) and then ligating it into the pNPTS138 vector(Materials and methods).

Using *spmB* knockout plasmid we deleted the *spmB* gene in the *ΔspmY* cells by a double homologous recombination method(Materials and methods). The positive clones were screened by polymerase chain reaction(PCR)(Figure 5A). Similarly, the *spmB* gene was deleted in *ΔspmX* cells(Figure 5B). Next, Using the same method we deleted the *spmA* gene in *ΔspmY* and *ΔspmX* cells (Figure 5C,5D).

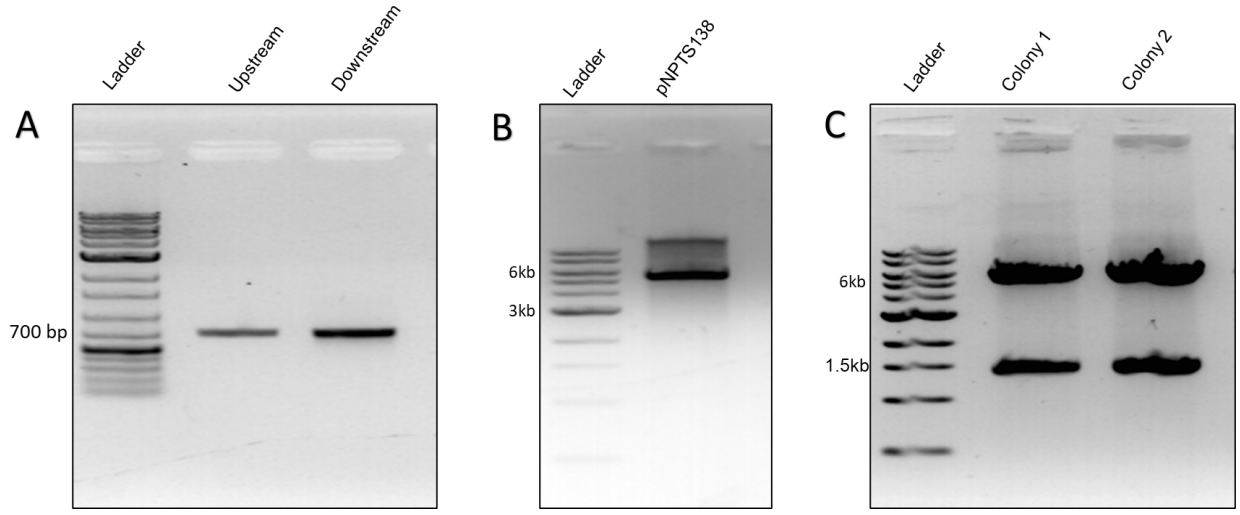


Figure 4: **Construction of *spmB* knockout plasmid**: 1% Agarose gel showing A) Amplified upstream and downstream fragments B) pNPTS138 vector digested using HindIII and EcoRI restriction enzymes. C) Confirmation of positive clones by isolating plasmid from positive colonies and then digesting it with HindIII and EcoRI restriction enzymes.

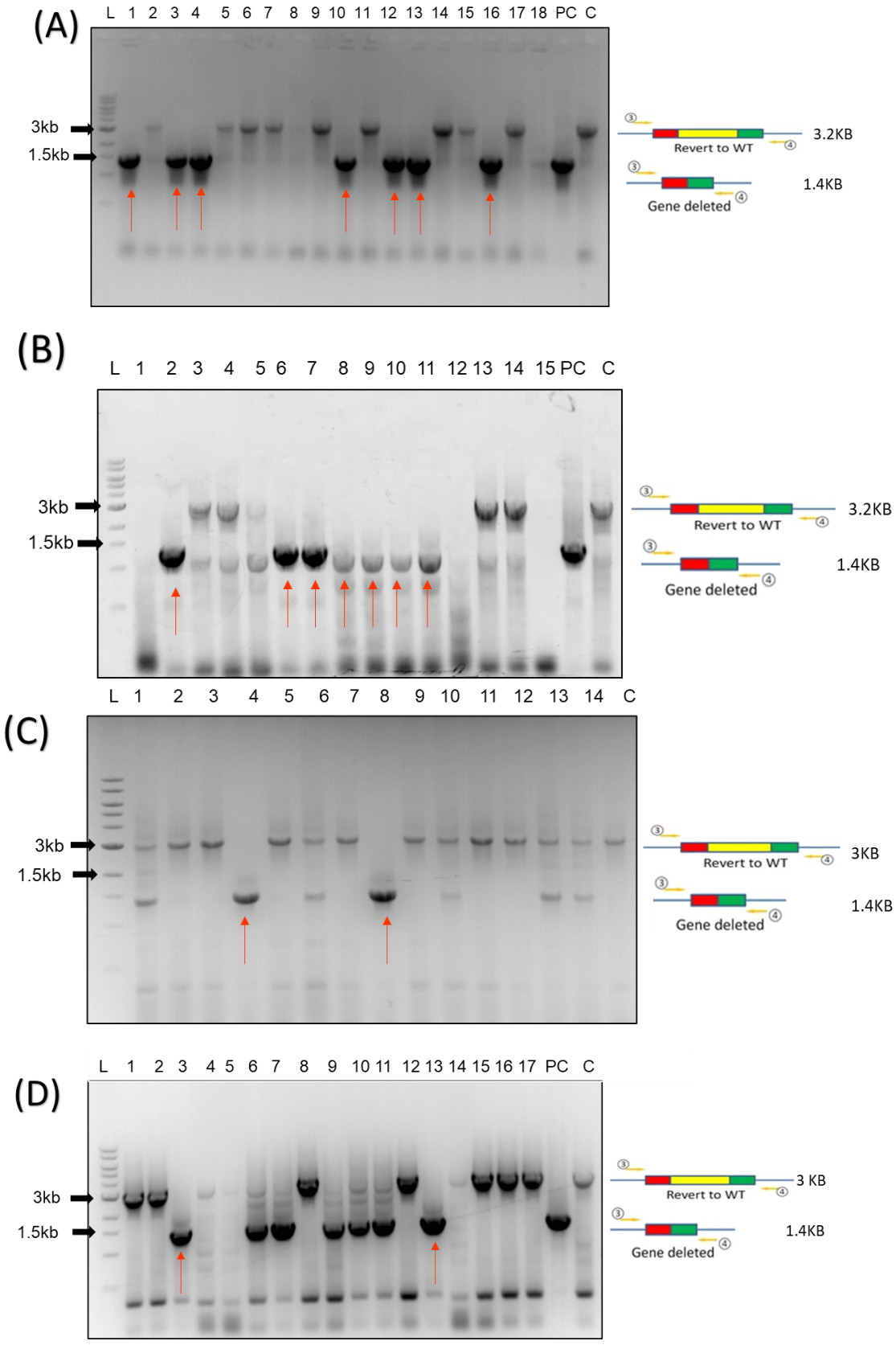

(A)
L 1 2 3 4 5 6 7 8 9 10 11 12 13 14 15 16 17 18 PC C
3kb
1.5kb
Revert to WT
3.2KB
Gene deleted
1.4KB
(B)
L 1 2 3 4 5 6 7 8 9 10 11 12 13 14 15 PC C
3kb
1.5kb
Revert to WT
3.2KB
Gene deleted
1.4KB
(C)
L 1 2 3 4 5 6 7 8 9 10 11 12 13 14 C
3kb
1.5kb
Revert to WT
3KB
Gene deleted
1.4KB
(D)
L 1 2 3 4 5 6 7 8 9 10 11 12 13 14 15 16 17 PC C
3kb
1.5kb
Revert to WT
3 KB
Gene deleted
1.4KB

Figure 5: 1 % Agarose gel showing colony PCR for A) *spmB* knockout in Δ*spmY* background. Colony number 1, 3, 4, 11, 13, 14, and 17 shows bands corresponding to knockouts B) *spmB* knockout in Δ*spmX* background. Colony number 2, 6, 7, 8, 9, 10 and 11 show bands corresponding to knockouts. C) *spmA* knockout in Δ*spmY* background. Colony number 4 and 8 show bands corresponding to knockouts D) *spmA* knockout in Δ*spmX* background. Colony number 3 and 13 show bands corresponding to knockouts. The red arrows point out the positive clones. The block diagram beside each gel image shows the graphical representation of the scenario when a gene is deleted or when a gene is not deleted. The knockout plasmid is used as a template for PCR as a positive control, whereas NA1000 genomic DNA was used as a template for PCR as a negative control. Abbreviations- Positive control(pc), control (c), ladder(L)

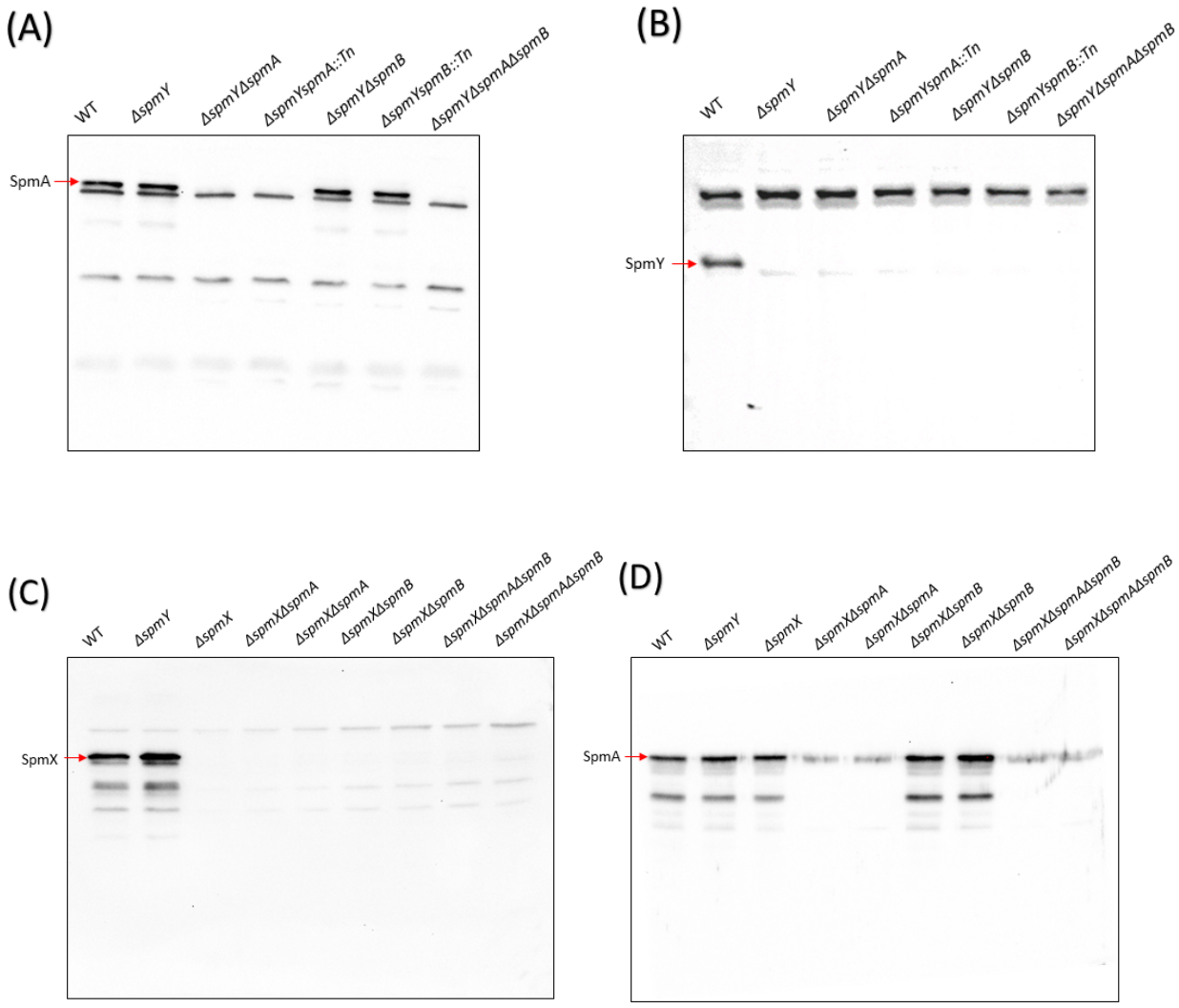


Figure 6: A) Immunoblot showing absence of SpmA in *ΔspmYΔspmA, ΔspmYspmA::Tn, ΔspmYspmB::Tn ΔspmYΔspmAΔspmB* cells. B) Immunoblot showing absence of SpmY in *ΔspmYΔspmA, ΔspmYspmA::Tn ΔspmYΔspmAΔspmB, ΔspmYspmA::Tn* cells. C) Immunoblot showing absence of

SpmX in *ΔspmXΔspmA, ΔspmXΔspmB, ΔspmYΔspmAΔspmB,* cells D) Immunoblot showing absence of SpmA in *ΔspmXΔspmA, ΔspmXΔspmAΔspmB* cells.

We validated knockouts by probing cell lysate on immunoblot with anti-SpmA antibodies(Figure 6A). No band corresponding to SpmA protein was observed in *spmA* knockout cells(Figure 6A). Immunoblot was also probed with anti-SpmY antibodies and no band corresponding to SpmY protein was observed in *ΔspmY, ΔspmYΔspmA, ΔspmYΔspmB, ΔspmYΔspmAΔspmB* cells(Figure 6B). Similarly, the knockouts in the *ΔspmX* background were validated by probing with anti-SpmX and anti-SpmA antibodies(Figure 6A, 6B).

Mutation in *spmA* or *spmB* specifically alleviates the phenotypic defects of Δ*spmY* cells

ΔspmY cells have division and motility defects due to which they are long and filamentous(Figure 7A). The transposon insertion in *spmA* and *spmB* not only rescued the motility defects in *ΔspmY* cells but also corrected for the division defects(Figure 3A). The *ΔspmYspmA::Tn* cells were significantly shorter as compared to the *ΔspmY* cells. Furthermore, they did not show any filamentation(Figure 7A). Deletion of *spmA* (*ΔspmA*) in *ΔspmY* cells phenocopied *ΔspmY*spmA*::Tn* mutant. The *ΔspmYΔspmA* cells were shorter than the *ΔspmY* cells(Figure 7A). When checked for the motility of the *ΔspmYΔspmA* cells, it was observed that deletion of *spmA* improved the motility of *ΔspmY* cells(Figure 8A).

Surprisingly, the deletion of *spmB* could not rescue the phenotypic defects of *ΔspmY* cells. Though the *ΔspmYspmB::Tn* mutants were short and motile, the *ΔspmYΔspmB* cells were long and filamentous (Figure 6A). We observed stalks emerging from both the poles of the *ΔspmYΔspmB* mutants which indicate loss of cellular asymmetry in these mutants, as seen in the case of *ΔspmY* cells(Figure 6A). Additionally, deletion of *spmB* did not correct for motility defects of *ΔspmY* cells(Figure 8A). This difference between the phenotype of *ΔspmYspmB::Tn* mutants and *ΔspmYΔspmB* mutants might arise due to the promoter present in transposon, which

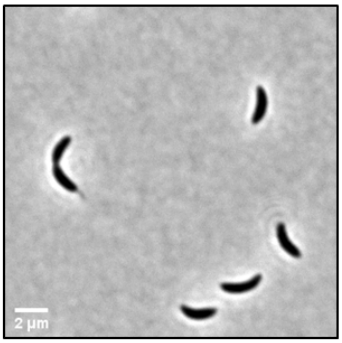
might change the expression of gene present upstream of *spmB*. Currently, this is being investigated in the lab independently.

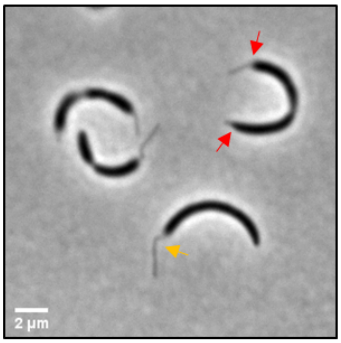
If the mutation in *spmA* and *spmB* correct defects in *ΔspmY* cells by correcting the defects in the TacA pathway, then it should also correct defects in *ΔspmX* cells given that SpmY acts downstream of SpmX in the TacA pathway(Janakiraman et al., 2016). Therefore, to check this we deleted *spmA* and *spmB* in the *Δspmx* background (Figure 5B, 5D). We observed that deletion of *spmA* in *Δspmx* cells resulted in only a partial rescue of *ΔspmX* phenotype while the deletion on spmB did not mitigate phenotypic defects in *ΔspmX* cells(Figure 7B). These results indicate that mutation of spmA and spmB might not be correcting the developmental defects in *ΔspmY* cells by correcting for the defects in the TacA pathway.

Even though the motility and the division defects in *ΔspmY* cells were rescued in *ΔspmYspmA::Tn* mutants, the cells have a long stalk which is a typical feature of the cells having hyperactivity of TacA (Figure 7A). Similarly, long stalks were observed in *ΔspmYspmA, ΔspmYspmB::Tn, and ΔspmYspmB* cells(Figure 7A). This further points out that TacA~P levels are high in these cells, suggesting that the mutation of *spmA* and *spmB* does not correct defects in the TacA pathway.

(A)

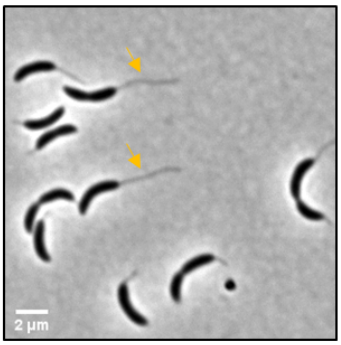
WT
(2.57±0.82µm)

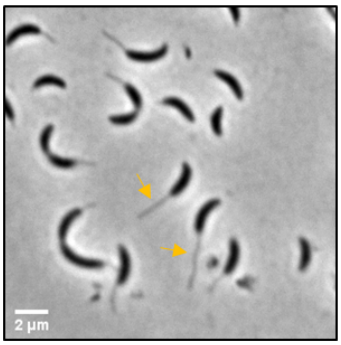




ΔspmY
(4.37±1.47µm)

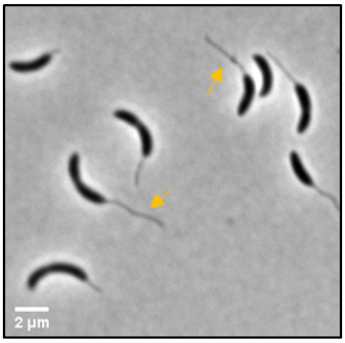
ΔspmYspmA::Tn
(2.58±0.73µm)

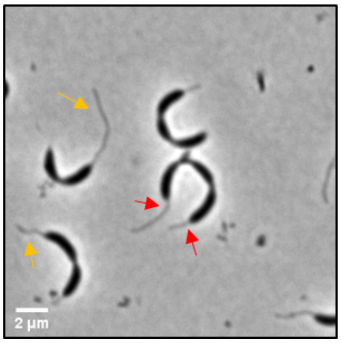




ΔspmYΔspmA
(2.87±1.15µm)

ΔspmYspmB::Tn
(2.53±0.81µm)

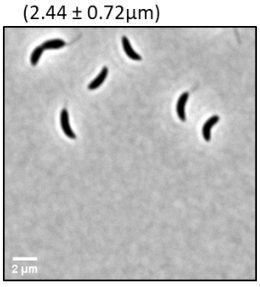




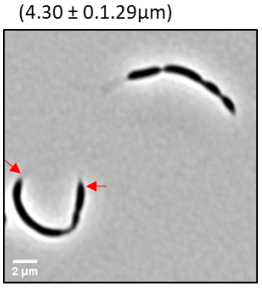
ΔspmYΔspmB
(3.55±1.13µm)

(B)

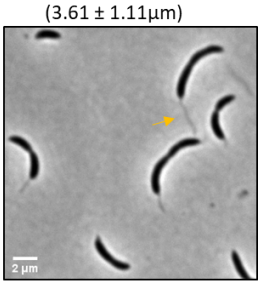
WT
(2.44 ± 0.72µm)



ΔspmX
(4.30 ± 0.1.29µm)



ΔspmXΔspmA
(3.61 ± 1.11µm)



ΔspmXΔspmB
(4.05 ± 1.23µm)

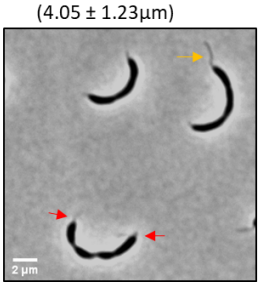


Figure 7: A) Phase-contrast microscopy images of WT, *ΔspmY, ΔspmYspmA::Tn, ΔspmYΔspmA, ΔspmYspmB::Tn, ΔspmYΔspmB* cells. Values given beside the image indicate mean cell length ± standard deviation of a minimum of 300 cells. B) Phase-contrast microscopy images of WT, *ΔspmY, ΔspmXΔspmA, ΔspmXΔspmB*. The red arrows indicate the ectopic stalks. The yellow arrows point out the long stalks in mutant cells. The experiments were performed at least five times independently. Values at the top of the image indicate mean cell length ± standard deviation of a minimum of 300 cells. Scale bar = 2 μm.

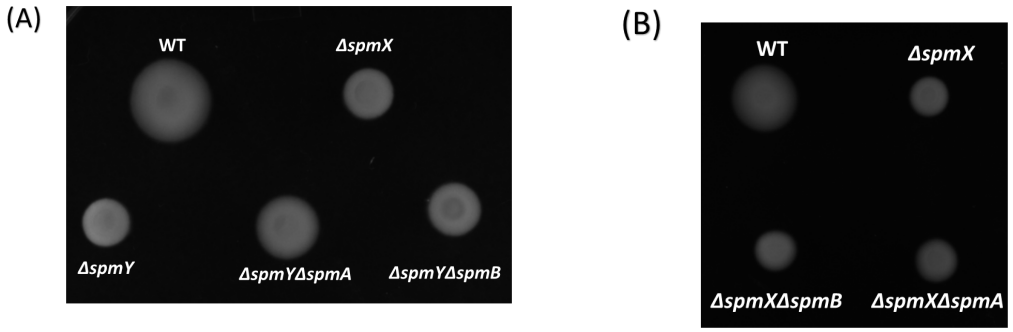


Figure 8: A) Soft agar(0.3%) plates showing the swarming motility of cells in WT, *ΔspmY, ΔspmX, ΔspmYΔspmA, ΔspmYΔspmB* genetic background. B) Motility assay of WT, *ΔspmX*, *ΔspmXΔspmA, ΔspmXΔspmB* cells on 0.3% agar plate. The experiments were performed at least five times independently.

Deletion of *spmA* or *spmB* does not correct the defects in the TacA pathway in *ΔspmY* cells

To further confirm the above results, we measured the activity of TacA using the β-Galactosidase assay. Given that TacA~P is required for activation of the *spmX* promotor(P_{spmX}), the β-Galactosidase assay was performed using the P_{spmX}-*lacZ* construct to measure the active level of TacA (TacA~P) in *ΔspmYΔspmA, ΔspmYΔspmB, ΔspmXΔspmA, ΔspmXΔspmB* strains. As expected, the activity of P_{spmX}-*lacZ* was higher in the *ΔspmYΔspmA* and *ΔspmYΔspmB* mutants as compared to WT cells(Figure 9A). Additionally, there was no significant difference in the P_{spmX}-*lacZ* activity in *ΔspmY* mutants and *ΔspmYΔspmA, ΔspmYΔspmB* mutants indicating higher levels of active TacA(TacA~P) in these cells(Figure 9A).

Similarly, we observed that P_{spmX}-*lacZ* activity is also high in *ΔspmXΔspmA* and *ΔspmXΔspmB* cells(Figure 9B). Furthermore, the P_{spmX}-*lacZ* activity in *ΔspmX*,

ΔspmXΔspmA and *ΔspmXΔspmB* showed a non-significant difference(Figure 9B). Taken together these findings support the conclusion that the deletion of *spmA* and *spmB* does not correct for the defects in the TacA pathway and the TacA~P levels.

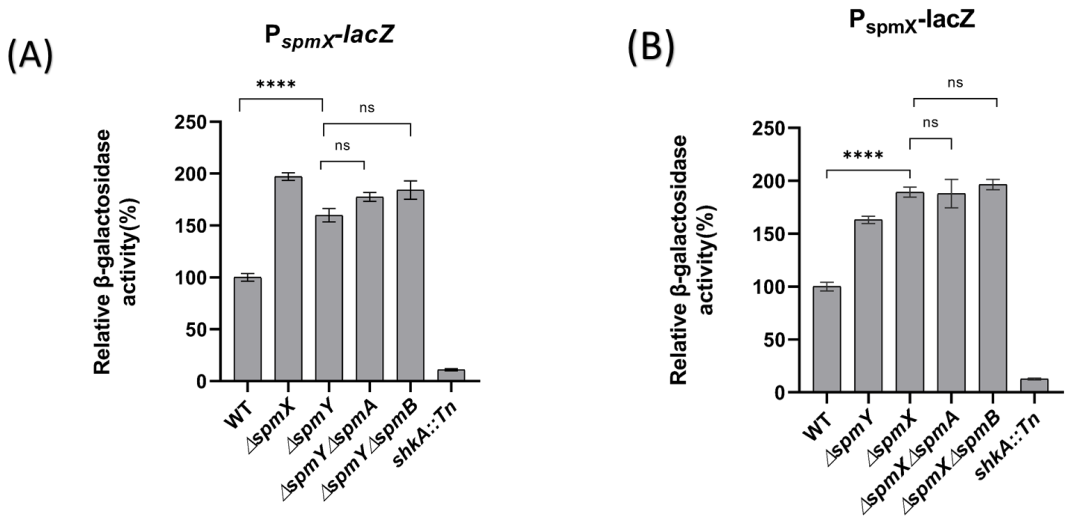


Figure 9: A) β-galactosidase activity(relative) of P_{spmX}-*lacZ* promoter-probe reporter in WT, *ΔspmX, ΔspmY, ΔspmYΔspmA, ΔspmYΔspmB, shkA*::Tn cells. B) β-galactosidase activity(relative) of P_{spmX}-*lacZ* promoter-probe reporter in WT, *ΔspmY, ΔspmX, ΔspmXΔspmA, ΔspmXΔspmB, shkA*::Tn cells. Values indicated in (A) and (B) are the average of three independent experiments, the error bars indicate standard error of mean (SEM). Statistical significance was calculated by paired t-test ; ****p < 0.0001; non-significant difference(ns).

Immunoprecipitation of SpmY

The above results suggest that the suppressor mutation in *ΔspmY* cells does not correct the hyperactivity of TacA. This does not answer 'How SpmY negatively regulated TacA', the question that we started with. To answer this question, we took another approach. We immunoprecipitated SpmY and analysed the proteins which co-immunoprecipitated with SpmY. If SpmY interacts with TacA or proteins that phosphorylate TacA, they will immunoprecipitate with SpmY. For this experiment, we expressed SpmY tagged at the C terminus with ALFA-tag to construct SpmY-ALFA. We then cloned *spmY* into the pRXMCS2-C-ALFA vector (Figure 10A, 10B, 10C).

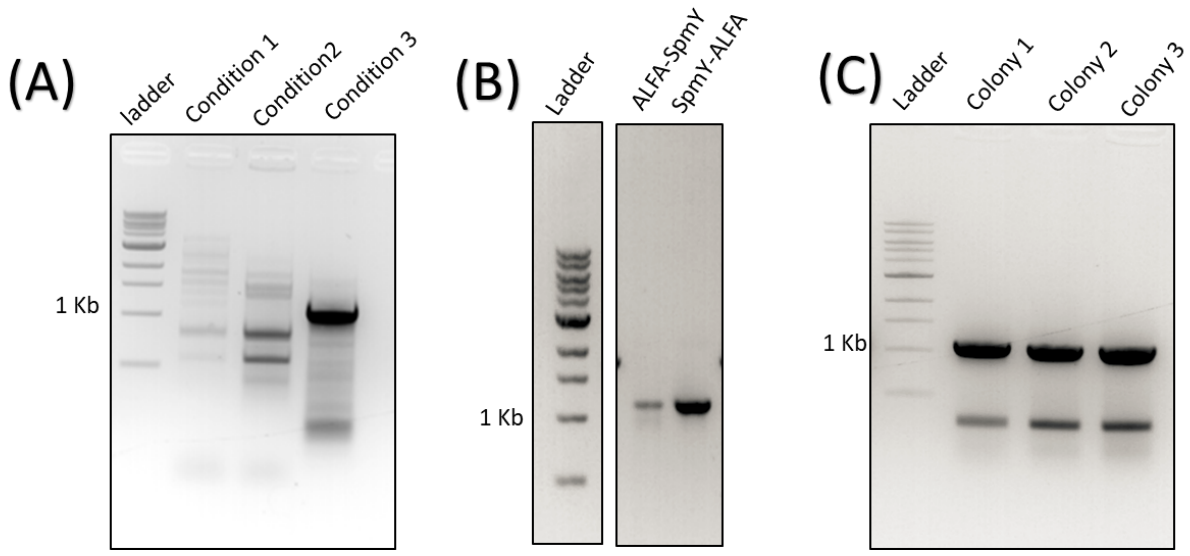


Figure 10: A) 1% agarose gel showing amplification of spmY in different PCR conditions with successfully amplified SpmY in lane number 4. B) 1% agarose gel showing digested ALFA-SpmY and SpmY-ALFA in 4th and 5th lane respectively. C) 1% agarose gel showing colony PCR result with lane number 3, 4, 5 showing positive colonies.

To check the steady-state level of SpmY-ALFA, *ΔspmY* cells containing SpmY-ALFA plasmid were induced with 0.3% xylose, and an equal amount of cells were pelletised. The samples were run on SDS-PAGE gel and then transferred to the PVDF membrane. The immunoblot was then probed with anti-SpmY antibodies. SpmY-ALFA(41.2 KD) band was observed in cell lysate *ΔspmY* cells expressing SpmY-ALFA(Figure 11). As expected, this band migrated slower than the SpmY band(39.5 KD) as observed in the WT cell lysate(Figure 11).

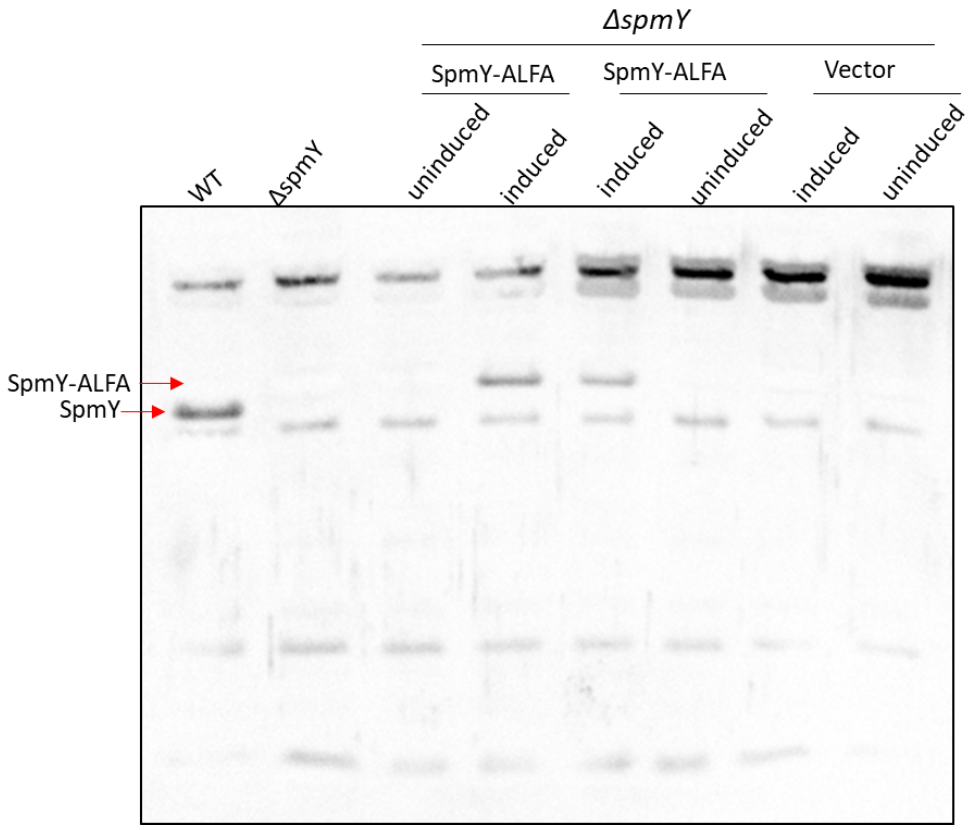


Figure 11: Western blot showing the steady-state level of SpmY. Lane 1 shows SpmY from WT (39.5 KD), and lane 5 and 6 show the band corresponding to SpmY-ALFA (41.2 KD) in the xylose induced cell extracts of *ΔspmY* cells harbouring *spmY*-ALFA plasmid.

After confirming steady-state levels of SpmY-ALFA, we went ahead with ALFA-pulldown, taking the empty vector as a control. To begin, a resin with an immobilised nanobody that recognises the ALFA tag was used to pull-down the SpmY-ALFA. Then by immunoblotting, the immunoprecipitated samples were probed using anti-SpmA antibodies to detect the presence of SpmA, and no significant difference was observed between SpmY-ALFA pulldown and empty vector control (Figure 12A). The same immunoblot was then probed with anti-TacA antibodies to check if the TacA interacts with SpmY. There was no significant difference between the SpmY-ALFA and the empty vector control (Figure 12B). Lastly, the blot was probed with

anti-SpmY antibodies and the concentration of SpmY-ALFA was found to be less (Figure 12C); therefore, we decided to repeat the pulldown with a culture of a larger volume.

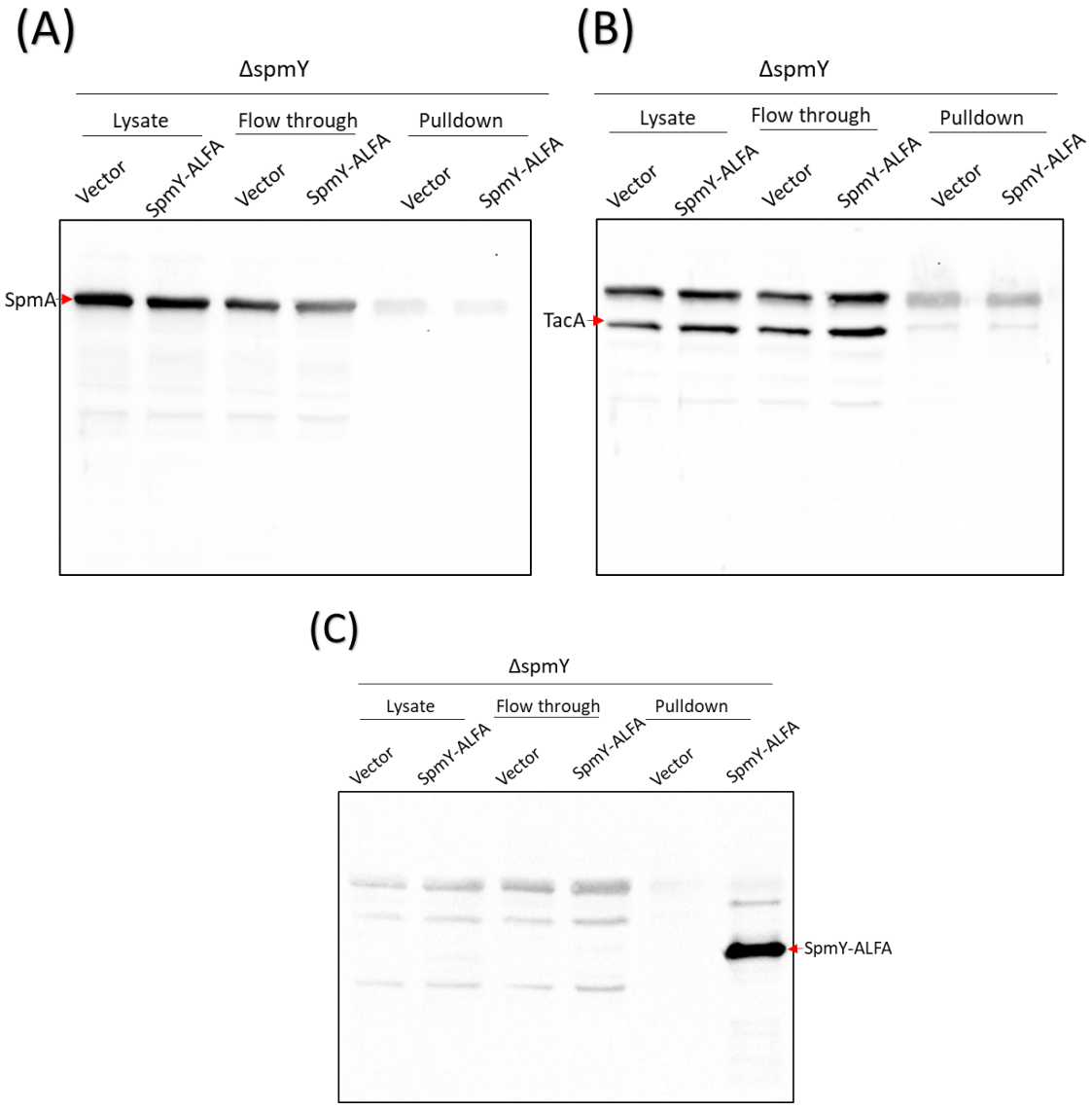


Figure 12: Immunoblot showing immunoprecipitated (IP) samples. SpmY-ALFA was immunoprecipitated from a lysate of *ΔspmY* cells expressing SpmY-ALFA from P_{xyl} on pRXMCS2. The extracts of *ΔspmY* cell harbouring the empty vector(pRXMCS2) were used as control. A) Immunoblot showing the levels of SpmA. B) Immunoblot showing the levels of TacA. C) Immunoblot showing the levels of SpmY-ALFA.

Pulldown was repeated using 500 ml of culture. Again, in this pulldown, the yield of SpmY-ALFA was less(Figure 13A). When probed with anti-SpmA antibodies it was observed that SpmY-ALFA pulldown and empty vector control are not significantly different (Figure 13C) but when probed with TacA, the signal from the TacA band was higher in SpmY-ALFA pulldown as compared to the empty vector pulldown. This suggests that there might be some interaction between SpmY and TacA. However, we were not able to confirm this observation in subsequent experiments.

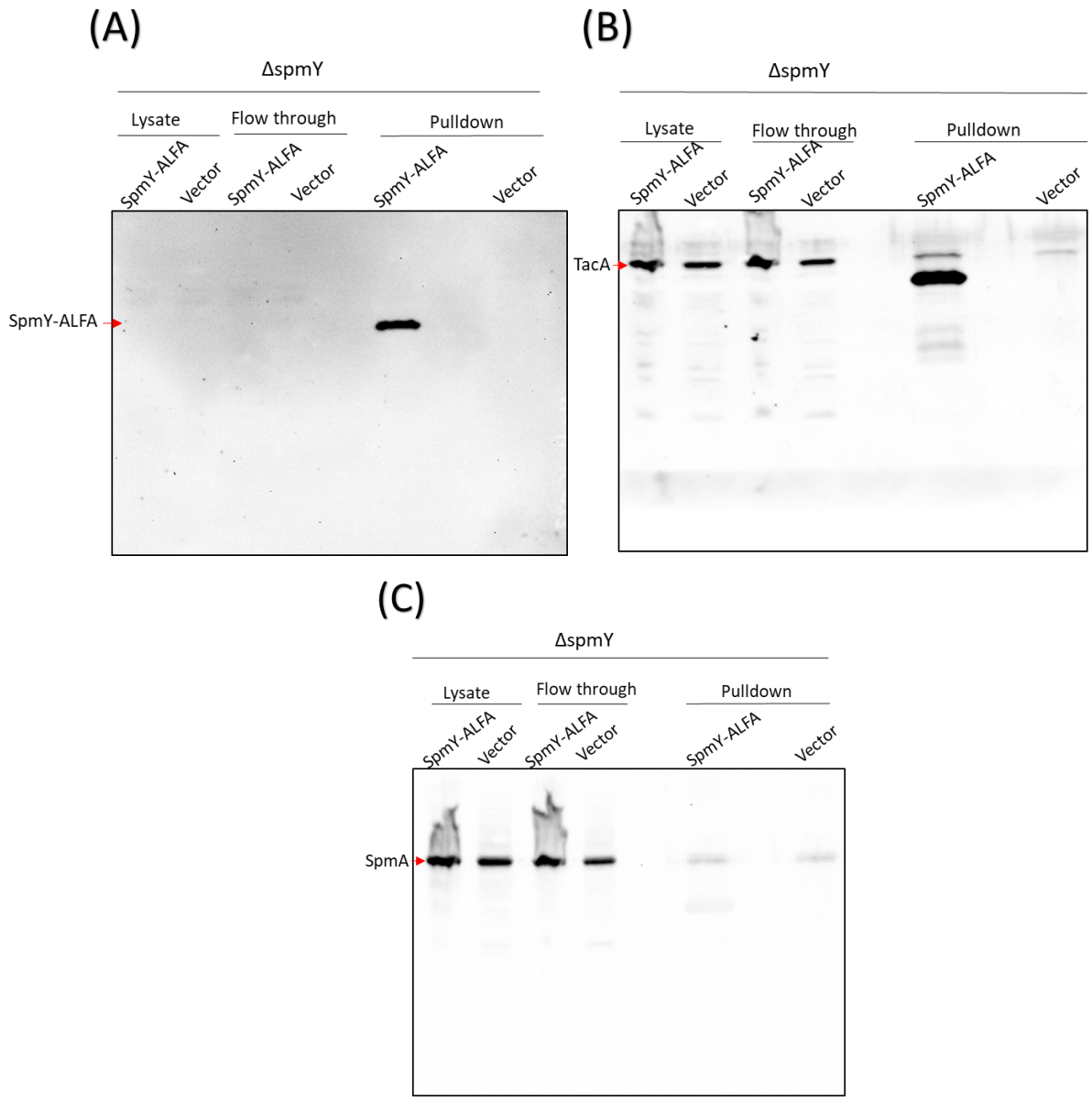


Figure 13: Immunoblot showing immunoprecipitated (IP) samples. SpmY-ALFA was immunoprecipitated from a lysate of Δ*spmY* cells expressing SpmY-ALFA from P*xyl* on pRXMCS2. The extracts of Δ*spmY* cell harbouring the empty vector(pRXMCS2) were used as control. A) Levels of SpmY when immunoblot was probed with anti SpmY antibodies. B) Levels of TacA when immunoblot was probed with anti-TacA antibodies. C) Levels of SpmA, when immunoblot was probed with anti-SpmA antibodies.

Attaching the ALFA tag to the C-terminus of SpmY might be making it unstable which might explain the low yield of SpmY-ALFA in previous pulldowns. To avoid this

problem, we decided to proceed with co-immunoprecipitation, using anti-SpmY antibodies. We immunoprecipitated SpmY by treating the extract from WT cells with anti-SpmY antibodies. The extract from *ΔspmY* cells were used as a control. Agarose protein-A beads were used to trap the antibody-SpmY complex and immunoprecipitate SpmY. The co-immunoprecipitated proteins were analysed using mass spectrometry. We analysed the mass spectrometry data with ProteinPilot software and a cutoff was applied such that only proteins with at least three peptides detected will be taken into consideration. We identified 102 proteins in an immunoprecipitated sample from WT cells, while in control we identified 54 proteins(Figure 14A,14B).

(A)

Unused (Conf) Cutoff	Proteins Detected	Proteins Before Grouping	Distinct Peptides
>2.0 (99)	134	139	733
>1.3 (95)	190	213	798
>0.47 (66)	229	251	858
Cutoff Applied: >3.0 (99.9%)	102	104	646

(B)

Unused (Conf) Cutoff	Proteins Detected	Proteins Before Grouping	Distinct Peptides
>2.0 (99)	73	74	374
>1.3 (95)	118	133	422
>0.47 (66)	131	148	446
Cutoff Applied: >3.0 (99.9%)	54	55	331

(C)

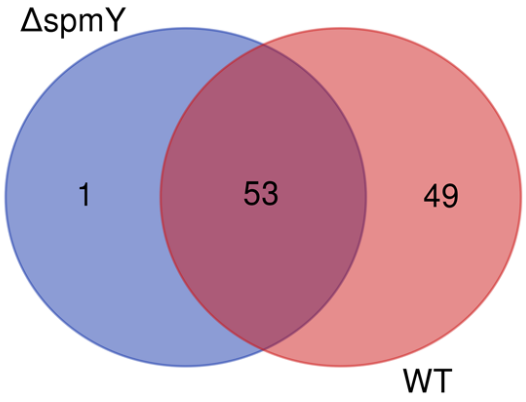
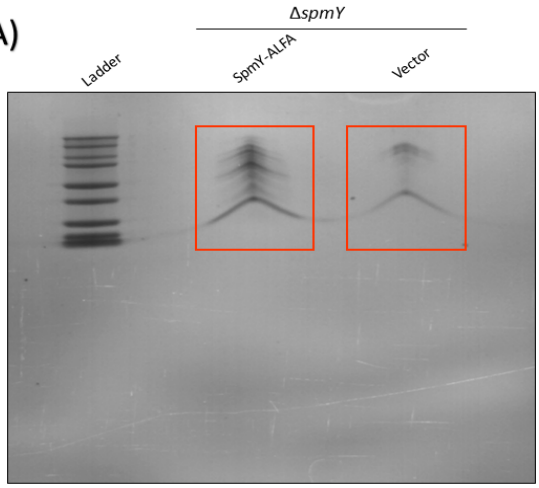


Figure 14: Native SpmY pulldown mass spectrometry result. A) Table listing the number of distinct peptides and proteins identified after mass spectrometry analysis of SpmY pulldown in WT cells. B) Table listing number of distinct peptides and proteins identified after mass spectrometry analysis of SpmY mock pulldown in *ΔspmY* cells. C) Venn diagram showing the overlapping proteins in SpmY pulldown in WT cells and in *ΔspmY* cells(control).

(A)



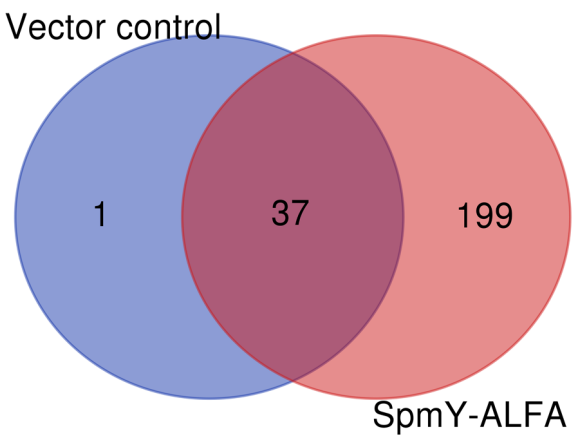
(B)

Unused (Conf) Cutoff	Proteins Detected	Proteins Before Grouping	Distinct Peptides
>2.0 (99)	773	811	5531
>1.3 (95)	917	967	5686
>0.47 (66)	995	1040	5775
Cutoff Applied: >3.0 (99.9%)	637	659	5271

(C)

Unused (Conf) Cutoff	Proteins Detected	Proteins Before Grouping	Distinct Peptides
>2.0 (99)	271	287	1686
>1.3 (95)	334	364	1777
>0.47 (66)	406	438	1900
Cutoff Applied: >3.0 (99.9%)	216	221	1536

(D)



(E)

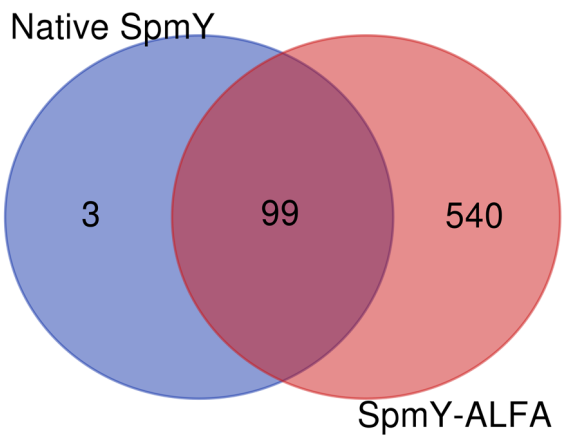


Figure 15: SpmY-ALFA pulldown mass spectrometry result. A) SDS-PAGE gel showing SpmY-ALFA pulldown sample and empty vector control sample. In SpmY-ALFA more proteins are seen as compared to vector control. The portion of gel marked by the red box was cut and sent for mass spectrometry analyses. B) Table listing number of distinct peptides and proteins identified after mass spectrometry analysis of SpmY-ALFA pulldown sample. C) Table listing number of distinct peptides and proteins identified after mass spectrometry analysis of empty vector pulldown sample. D) Venn diagram showing the overlapping proteins in SpmY-ALFA pulldown and in empty vector control with at least 25% coverage. E) Venn diagram showing the overlapping proteins in pulldown of native SpmY(first pulldown) and in SpmY-ALFA pulldown(second pulldown).

We also proceeded with ALFA tag pulldown, and then mass spectrometry analysis. 650 proteins were identified from the extracts of *ΔspmY* cells expressing

SpmY-ALFA from xylose inducible promoter while in control cells harbouring the empty vector encoding ALFA, 250 proteins were identified(Figure 15A,15B). To increase the confidence of our analysis we further narrowed down proteins detected, we only considered proteins that have at least 25% peptide coverage in mass spectrometry(Figure 15D). The difference in the number of proteins detected in these two pulldowns might be attributed to the culture volume used for the pulldown. In native SpmY pulldown, we used 250 ml of culture while for SpmY-ALFA pulldown we used 1000ml culture. Nevertheless, almost all proteins which were present in the native SpmY pulldown were also present in the SpmY-ALFA pulldown indicating the robustness of pulldown and mass spectrometry analysis(Figure 15E).

Among these proteins, we decide further to investigate protein citrate synthase(henceforth CitA). The CitA is a Krebs cycle enzyme, but recently it has been shown that besides its enzymatic role, it also plays a role in cell cycle regulation, thereby connecting the central metabolism and the bacterial cell cycle(Bergé et al., 2020). CitA imparts its function by modulating the activity of a crucial cell cycle regulatory protein CtrA, the master transcriptional regulator that keeps cells in the G1 phase of the cell cycle. Deletion of *citA* results in the accumulation of the active form of CtrA; also, in *ΔcitA* cells, ctrA becomes less prone to degradation than WT cells (Bergé et al., 2020). Interestingly, the previously identified CtrA(T170A) allele of ctrA, which has gain of function mutation, increases the activity of CtrA dependent promoters and when expressed in *ΔspmX* and *ΔspmY* cells it restores the motility defects of these cells(Janakiraman et al., 2016, Fumeaux et al., 2014). Based on this information, we hypothesised that SpmY might be regulating the activity of CtrA through CitA. To check this, We constructed *spmYcitA* double mutant(*ΔspmYcitA::Tn)* and *spmXcitA* double mutant(*ΔspmXcitA::Tn)*. As expected, the mutation in citA was able to restore the motility in *ΔspmX* and *ΔspmY* cells(Figure 16), suggesting that mutation in citA might be restoring motility in *ΔspmX* and *ΔspmY* cells through CtrA. The *ΔspmXcitA::Tn* mutant cells were more motile as compared to the *ΔspmY citA::Tn,* in line with the previous observation that *ΔspmXctrA(T170A)* cells were more motile than *ΔspmY*ctrA(T170A) cells(Janakiraman et al., 2016). This suggests that SpmY might be regulating CtrA through CitA, however, this needs further investigation.

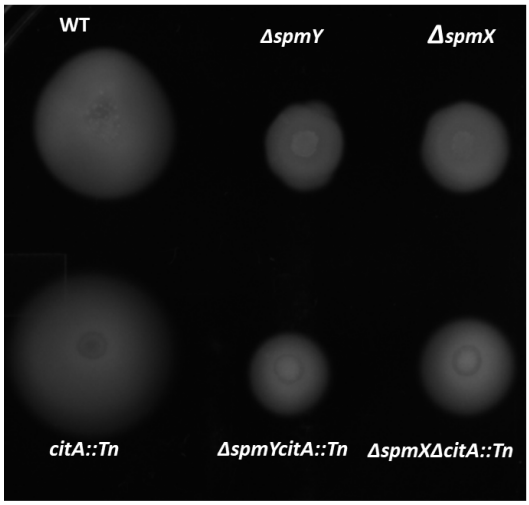


Figure 16: Swarm plate showing the motility of cells in WT, *ΔspmY, ΔspmX, citA::Tn, ΔspmYΔcitA::Tn, ΔspmX citA::Tn* genetic background. The experiments were performed at least three times independently.

CONCLUSION

Previous studies have shown that SpmY negatively regulates the activity of TacA, and the deletion of *spmY* results in hyperactivity of TacA, giving rise to developmental defects in *ΔspmY* cells. Here, we show that the deletion of *spmA* cures the developmental defects in *ΔspmY* cells but not in *ΔspmX* cells implying that the deletion of *spmA* might not correct the developmental defects in *ΔspmY c*ells by correcting defects in the TacA pathway. To confirm this, we measured P_{spmX}-*lacZ* activity in double mutants by β-Galactosidase assay. We show that P_{spmX}-*lacZ* activity remains high in *ΔspmY, ΔspmX*, *ΔspmYΔspmA*, *ΔspmYΔspmB*, *ΔspmXΔspmA*, *ΔspmXΔspmB*, suggesting that the mechanism of action of SpmA is independent of the TacA pathway.

Furthermore, we immunoprecipitated SpmY-ALFA and analysed the proteins that co-immunoprecipitated with SpmY by mass spectrometry analysis. We identified many known cell cycle regulating proteins that interact with SpmY. Among these proteins, we further investigated an important Kreb cycle enzyme CitA. This protein also regulates the cell cycle by modulating the activity of master cell cycle regulator CtrA. To examine the role of CitA, we mutated *citA* in *ΔspmX* and *ΔspmY* cells, and we show that the mutation in *citA* in *ΔspmX* and *ΔspmY* background restores the motility, possibly through CtrA. To test if the restoration of motility in these cells is due to a change in the levels of the active form of CtrA, the activity of CtrA dependent promoters can be measured in *ΔspmX*, *ΔspmY*, *citA::Tn ΔspmXcitA::Tn*, *ΔspmYcitA::Tn* cells which will give us insight into the regulation of CtrA by SpmY.

In addition to CitA, studies on other proteins identified in pulldown need to be further pursued. We identified proteins Mucr1 and Mucr2 as interacting partners of SpmY. The Mucr1 and Mucr2 are known to inhibit CtrA activated promoters in the G1 phase, including TacA; it also acts positively on the expression of CtrA. It will be worth probing the effect of SpmY-MucR interaction on CtrA as well as on CtrA activated promoters.

REFERENCES

Bergé, M., Pezzatti, J., González-Ruiz, V., Degeorges, L., Mottet-Osman, G., Rudaz, S., and Viollier, P.H. (2020). Bacterial cell cycle control by citrate synthase independent of enzymatic activity. ELife *9*, e52272.

Biondi, E.G., Skerker, J.M., Arif, M., Prasol, M.S., Perchuk, B.S., and Laub, M.T. (2006). A phosphorelay system controls stalk biogenesis during cell cycle progression in Caulobacter crescentus. Mol. Microbiol. *59*, 386–401.

Curtis, P.D., and Brun, Y.V. (2010). Getting in the Loop: Regulation of Development in Caulobacter crescentus. Microbiol. Mol. Biol. Rev. MMBR *74*, 13–41.

Degnen, S.T., and Newton, A. (1972). Chromosome replication during development in Caulobacter crescentus. J. Mol. Biol. *64*, 671–680.

Ducret, A., Quardokus, E.M., and Brun, Y.V. (2016). MicrobeJ, a tool for high throughput bacterial cell detection and quantitative analysis. Nat. Microbiol. *1*, 1–7.

Fumeaux, C., Radhakrishnan, S.K., Ardissone, S., Théraulaz, L., Frandi, A., Martins, D., Nesper, J., Abel, S., Jenal, U., and Viollier, P.H. (2014). Cell cycle transition from S-phase to G1 in Caulobacter is mediated by ancestral virulence regulators. Nat. Commun. *5*, 4081.

Hung, D.Y., and Shapiro, L. (2002). A signal transduction protein cues proteolytic events critical to Caulobacter cell cycle progression. Proc. Natl. Acad. Sci. U. S. A. *99*, 13160–13165.

Jacobs, C., Hung, D., and Shapiro, L. (2001). Dynamic localization of a cytoplasmic signal transduction response regulator controls morphogenesis during the Caulobacter

cell cycle. Proc. Natl. Acad. Sci. U. S. A. *98*, 4095–4100.

Janakiraman, B., Mignolet, J., Narayanan, S., Viollier, P.H., and Radhakrishnan, S.K. (2016). In-phase oscillation of global regulons is orchestrated by a pole-specific organizer. Proc. Natl. Acad. Sci. *113*, 12550–12555.

Jonas, K., Chen, Y.E., and Laub, M.T. (2011). Modularity of the Bacterial Cell Cycle Enables Independent Spatial and Temporal Control of DNA Replication. Curr. Biol. *21*, 1092–1101.

Kaczmarczyk, A., Hempel, A.M., von Arx, C., Böhm, R., Dubey, B.N., Nesper, J., Schirmer, T., Hiller, S., and Jenal, U. (2020). Precise timing of transcription by c-di-GMP coordinates cell cycle and morphogenesis in Caulobacter. Nat. Commun. *11*, 816.

Laub, M.T., McAdams, H.H., Feldblyum, T., Fraser, C.M., and Shapiro, L. (2000). Global analysis of the genetic network controlling a bacterial cell cycle. Science *290*, 2144–2148.

Laub, M.T., Shapiro, L., and McAdams, H.H. (2007). Systems Biology of Caulobacter. Annu. Rev. Genet. *41*, 429–441.

Matroule, J.-Y., Lam, H., Burnette, D.T., and Jacobs-Wagner, C. (2004). Cytokinesis monitoring during development; rapid pole-to-pole shuttling of a signaling protein by localized kinase and phosphatase in Caulobacter. Cell *118*, 579–590.

McGrath, P.T., Iniesta, A.A., Ryan, K.R., Shapiro, L., and McAdams, H.H. (2006). A dynamically localized protease complex and a polar specificity factor control a cell cycle master regulator. Cell *124*, 535–547.

Pd, C., and Yv, B. (2010). Getting in the loop: regulation of development in Caulobacter crescentus. Microbiol. Mol. Biol. Rev. MMBR *74*.

Pierce DL, et al. (2006) Mutations in DivL and CckA rescue a divJ null mutant of Caulobacter crescentus by reducing the activity of CtrA. J Bacteriol 188(7):2473–2482.
m
Quon, K.C., Marczynski, G.T., and Shapiro, L. (1996). Cell Cycle Control by an Essential Bacterial Two-Component Signal Transduction Protein. Cell *84*, 83–93.

Quon, K.C., Yang, B., Domian, I.J., Shapiro, L., and Marczynski, G.T. (1998). Negative control of bacterial DNA replication by a cell cycle regulatory protein that binds at the chromosome origin. Proc. Natl. Acad. Sci. U. S. A. *95*, 120–125.

Radhakrishnan, S.K., Thanbichler, M., and Viollier, P.H. (2008). The dynamic interplay between a cell fate determinant and a lysozyme homolog drives the asymmetric division cycle of Caulobacter crescentus. Genes Dev. *22*, 212–225.

Wheeler, R.T., and Shapiro, L. (1999). Differential localization of two histidine kinases controlling bacterial cell differentiation. Mol. Cell *4*, 683–694.